Self-induced stochastic resonance in excitable systems

Cyrill B. Muratov[a],[*], Eric Vanden-Eijnden[b], Weinan E[c]

[a] *Department of Mathematical Sciences, New Jersey Institute of Technology, Newark, NJ 07102, USA*
[b] *Courant Institute of Mathematical Sciences, New York University, New York, NY 10012, USA*
[c] *Department of Mathematics and PACM, Princeton University, Princeton, NJ 08544, USA*

Abstract

The effect of small-amplitude noise on excitable systems with strong time-scale separation is analyzed. It is found that vanishingly small random perturbations of the fast excitatory variable may result in the onset of a deterministic limit cycle behavior, absent without noise. The mechanism, termed self-induced stochastic resonance, combines a stochastic resonance-type phenomenon with an intrinsic mechanism of reset, and no periodic drive of the system is required. Self-induced stochastic resonance is different from other types of noise-induced coherent behaviors in that it arises away from bifurcation thresholds, in a parameter regime where the zero-noise (deterministic) dynamics does not display a limit cycle nor even its precursor. The period of the limit cycle created by the noise has a non-trivial dependence on the noise amplitude and the time-scale ratio between fast excitatory variables and slow recovery variables. It is argued that self-induced stochastic resonance may offer one possible scenario of how noise can robustly control the function of biological systems.
© 2005 Elsevier B.V. All rights reserved.

Keywords: Self-induced stochastic resonance; Coherence; Excitable systems; Large deviations; Noise-controlled

1. Introduction

Small random perturbations may have dramatic effects on dynamical systems and lead to the emergence of new dynamical behaviors which, surprisingly, can be deterministic in suitable limits [1]. Stochastic resonance is a well-known example [4,14]. A system driven by a weak periodic forcing will oscillate precisely with the period of the driving force in the presence of van-

ishingly small noise, whereas no such oscillation arises in the absence of noise. The periodic forcing changes which state is temporarily the most favorable energetically. Due to the noise, the system is able to reach this most favorable state by activated hopping events. The rate of the hopping depends mainly on the energy barrier to be crossed [3,6], and the barrier height varies in time due to the forcing. As a result, in a suitable limit as the period of the forcing goes to infinity and the amplitude of the noise to zero, the hopping takes place precisely when its rate matches the frequency of the driving force. This is the resonance phenomenon

* Corresponding author. Tel. +1 973 596 5833.
  E-mail address: muratov@njit.edu (C.B. Muratov).

whose net effect is a synchronization of the system with the forcing.

In this standard mechanism of stochastic resonance, the periodic forcing plays an essential role. Yet in recent years there has been numerical and experimental evidence that small random perturbations can also trigger transition to a deterministic periodic behavior even in the absence of periodic drive on the system. The corresponding mechanisms have been termed *autonomous stochastic resonance* [5,4,14] or *coherence resonance* [8,13]. They both arise in systems close to the threshold of bifurcation toward a periodic behavior. Above the bifurcation threshold, a limit cycle is present, but below threshold the intrinsic oscillation is only a transient feature observed while the system relaxes toward its equilibrium state. In such situations, the noise can temporarily push the system above the bifurcation threshold and thereby trigger a cycle. If the period of this cycle is much larger than the time-scale over which it is triggered by the noise, the ratio between the variance of the period and its mean is very small, i.e. the phenomenon displays a high degree of coherence. The resonance phenomenon in these mechanisms refers to the possibility to optimize the degree of coherence by adjusting the amplitude of the noise, which is quite different from its original meaning in standard stochastic resonance. In particular, both in autonomous stochastic resonance and in coherence resonance the time scale associated with the rate of noise-activated hopping does not have to match the intrinsic periodic time-scale of the system (it just has to be smaller than this time-scale to guarantee coherence). As a result, noise plays a rather passive role in these mechanisms. In addition, the constraint that the system be close to bifurcation requires fine-tuning of the control parameters. Thus, one may wonder if there is a more robust way by which noise can create deterministic periodic behavior in the absence of periodic driving force.

In this paper, we show that there exists indeed a robust mechanism, which we term *self-induced stochastic resonance*, by which small noise can trigger transition to a deterministic periodic behavior in systems away from bifurcation threshold, i.e. in a parameter regime where the zero-noise (deterministic) dynamics of the system does not display a limit cycle dynamics nor even its precursor. In addition, we show that the noise amplitude works as a control parameter for the coherent motion, hence the noise plays a truly constructive role in the deterministic dynamics it initiates. A similar mechanism has been reported recently by Freidlin in the pioneering paper [2]. Here we show its ubiquity in randomly perturbed excitable systems. (Self-induced stochastic resonance may, for instance, explain the results observed in the numerical experiments with the FitzHugh–Nagumo model performed in [15]).

Excitable systems arise in a wide variety of areas which include climate dynamics, chemical reactions, lasers, ion channels, nerve cells, neural systems, cardiovascular tissues, etc. and are especially common in biology [7–9]. One can think of them as dynamical systems possessing a rest state, an excited state, and a recovery state. In the absence of perturbations, an excitable system remains in the rest state. Small perturbations create only small amplitude linear responses. Larger perturbations, however, cause large-amplitude dynamical excursions during which the system goes to its excited state, then its recovery state, before returning to the rest state. Generally, the excited phase is fast whereas the recovery phase is slow because they arise as a result of the competition between positive and negative feedbacks operating on very different time-scales. As a result, the slow recovery motion in an excitable system can generally be described as a motion on a slow manifold that the system quickly reaches after a large excursion in the excited state.

We shall be interested in excitable systems whose excitatory variables are perturbed by small amplitude random perturbations. In these situations, we show that noise systematically triggers a new large excursion while the system is in the slow recovery state. The trigger mechanism involves a barrier crossing event by which the system escapes the slow manifold associated with the recovery state and whose rate depends on the position of the system on this manifold. As a result, the hopping always arises precisely when its rate matches the recovery time-scale. This is the stochastic resonance part of the mechanism. It is combined with a mechanism of reset provided by the excited state which mitigates the periodic forcing necessary in standard stochastic resonance and instead makes it self-induced. Indeed, after the large excursion in the excited state triggered by the hopping event, the system goes back to the state of slow recovery motion and the phenomenon can repeat itself over and over again. The result is the emergence of a deterministic limit cycle

induced by the noise whose amplitude and frequency are controlled by a parameter involving the amplitude of the noise and the ratio between the fast excitatory and the slow recovery time-scales.

The remainder of this paper is organized as follows. In Section 2 we explain the mechanism of self-induced stochastic resonance in the context of excitable system. We establish in which limit the mechanism arises and express the period of the limit cycle in terms of the noise amplitude and the ratio of time-scales in the system. In Section 3 we demonstrate the feasibility of the mechanism on the example of the Brusselator. In this system, a complete analysis is possible which we corroborate by a series of careful numerical experiments to illustrate how the coherence of the mechanism can be made arbitrarily high, how the noise can be used as a control parameter, etc. In Section 4 we compare self-induced stochastic resonance with coherence resonance to stress the differences between the two. Finally, some concluding remarks are given in Section 5.

2. The general mechanism of self-induced stochastic resonance

A generic excitable system consists of a set of excitatory and recovery variables, denoted, respectively by u and v, whose dynamics is governed by:

$$\begin{cases} \dot{u} = f(u, v) + \sqrt{\varepsilon}\eta, \\ \dot{v} = \alpha g(u, v). \end{cases} \qquad (1)$$

Here f and g are the nonlinearities, α is the ratio of the time-scales, and we have added some external noise η with amplitude ε perturbing the excitatory variables. The noise may have different physical origins. Here we will assume that η is external white-noise, i.e. a Gaussian process with mean zero and covariance:

$$\langle \eta(t)\eta(t') \rangle = \delta(t - t') \qquad (2)$$

different kinds of noise can be used and lead to qualitatively similar results.

When $\alpha \ll 1$, there is a large time-scale separation in the deterministic part of the dynamics governed by f and g. This is consistent with the excitatory variables u being fast and the recovery variables v being slow. Thus, the large excursions in the excited state
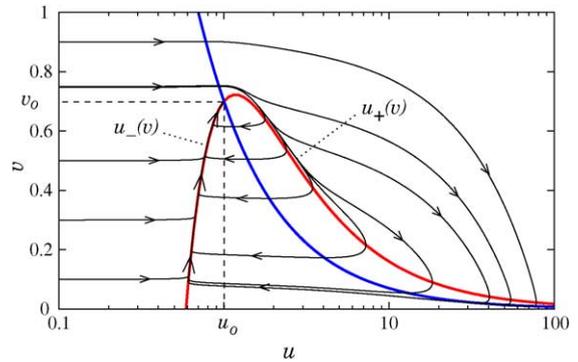

Fig. 1. Deterministic flow generated by (6). Here $A = 0.7$ and $\alpha = 0.01$. The thick curves are the u- and v-nullclines, respectively. The slow manifold of the recovery state is the $u_-(v)$ portion of the u-nullcline. The excited state corresponds to the part of the phase space to the right of the $u_+(v)$ portion of the u-nullcline. Note that u is shown on a logarithmic scale.

arise on the time-scale of order 1, and their dynamics is governed by the equation for u in Eq. (1) with v frozen (except, perhaps, in some part of the excursion when u turns over to go back to the recovery state, see below). The recovery state corresponds to a slow motion on the manifold defined by the stable solution branch of $f(u, v) = 0$ containing the rest state defined by $f(u, v) = g(u, v) = 0$ (see Fig. 1 for an illustration). In the absence of the noise, the excited state can only be a transient state, and the trajectory quickly approaches the slow manifold of the recovery state, and then proceeds on the time-scale α^{-1} along this manifold and into the globally attracting steady state.

With the introduction of the noise, the situation changes. The trajectory may leave the recovery state and go back to the excited state by escaping the slow manifold in the u direction via a noise-activated process. We will assume that for small noise, $\varepsilon \ll 1$, such process happens at Kramers rate [3,6]:

$$k = \nu \exp\left(\frac{-\Delta V(v)}{\varepsilon}\right) \ll 1, \qquad (3)$$

where $\Delta V(v)$ is some v-dependent energy barrier to be crossed to initiate the escape from the slow manifold, and ν is some characteristic frequency independent of ε. As a result, the system will perform an excursion in the excited state driven mainly by the deterministic part of the dynamics. After this excursion, the trajectory lands again somewhere on the slow manifold of the

recovery motion. The dynamics can then proceed along the slow manifold until another escape happens, and so on. This process may lead to a truly deterministic limit cycle in a suitable limit because of the following two mechanisms.

2.1. Resonance mechanism

The interplay between the escape events and the motion along the slow manifold requires that their time-scales be comparable. Assume that the energy barrier $\Delta V(v)$ in Eq. (3) decreases as one approaches the steady state by the dynamical path along the slow manifold (this amounts to assuming that the escape events become easier as the system approaches the steady state). Then by Eq. (3), the escape rate is a very rapidly increasing function of v when ε is small. Suppose that $\varepsilon, \alpha \to 0$ in a way that:

$$\varepsilon \log \alpha^{-1} \to \beta \tag{4}$$

for some finite β. Then escape from the slow manifold will occur with probability one at the point $v = v_\star$ on this manifold, where $v_\star$ satisfies:

$$\Delta V(v_\star) = \beta, \tag{5}$$

provided that this equation has a solution on the accessible part (i.e. the stable branch) of the slow manifold. For small but nonzero α and ε, escape occurs with probability close to one in the vicinity of the point $v = v_\star$ where $\Delta V(v_\star) = \varepsilon \log \alpha^{-1}$. Indeed, before v reaches $v_\star$, the slow recovery motion is so much faster than the escape rate that the system has no time to hop before it reaches $v_\star$. But as soon as v has passed $v_\star$, the escape rate becomes so much faster than the recovery motion that the system must hop. Thus, the matching of time-scales implied by (5) is precisely the resonance mechanism in standard stochastic resonance [1,14].

2.2. Reset mechanism

This is inherent to the excitable character of the system. After a large excursion in the excited state initiated from $v_\star$, the trajectory returns to the slow manifold at a point which leads again to $v_\star$ by the slow recovery motion. Then the process will repeat itself indefinitely in a sequence of recovery and excited states and the dynamics of the system will indeed be a limit cycle.

The mechanism described above does not require the system to be close to bifurcation, and therefore it is robust against parameter changes as long as (5) defines an accessible point on the slow manifold. In addition, since the dynamics in the recovery state is much slower than the one in the excited state, the period of the limit cycle will be dominated by the time it takes the system to go from the point it lands on at the slow manifold to $v_\star$ where it leaves it again. But since $v_\star$ depends on the amplitude of the noise ε and the ratio of time-scale α through (5), both α and ε can be used as control parameters for the period of the limit cycle.

3. The Brusselator

To demonstrate the feasibility of the self-induced stochastic resonance mechanism discussed in Section 2, we will consider the Brusselator [11]:

$$\begin{cases} \dot{u} = 1 + u^2 v - (1 + A)u + \sqrt{\varepsilon}\eta, \\ \dot{v} = \alpha(Au - u^2 v), \end{cases} \tag{6}$$

where u and v are scalars and A is a control parameter. This is of the form (1) for the nonlinearities $f = 1 + u^2 v - (1 + A)u$ and $g = Au - u^2 v$.

The Brusselator is a prototypical excitable system when $\alpha \ll 1$ and $A < 1$. This can be seen from its phase portrait shown in Fig. 1 for a particular choice of the parameters. When $A < 1$, the nullclines of (6) intersect on the stable branch of the u-nullcline, so the flow is always into the unique equilibrium point

$$(u_0, v_0) = (1, A). \tag{7}$$

Note that the slow manifold of the recovery state is essentially the part of the u-nullcline located at the left of the v-nullcline (see Fig. 1). It is also clear from the figure that sufficiently large increases in the u variable away from equilibrium will result in large excursions into the excited state. For $A > A_\omega$, where

$$A_\omega = 1 + \alpha, \tag{8}$$

the system exhibits a Hopf bifurcation: the steady state $(u_0, v_0) = (1, A)$ becomes unstable and a limit cycle emerges even in the absence of noise.

We begin by presenting results of the numerical simulations of Eq. (6) with a representative set of values of
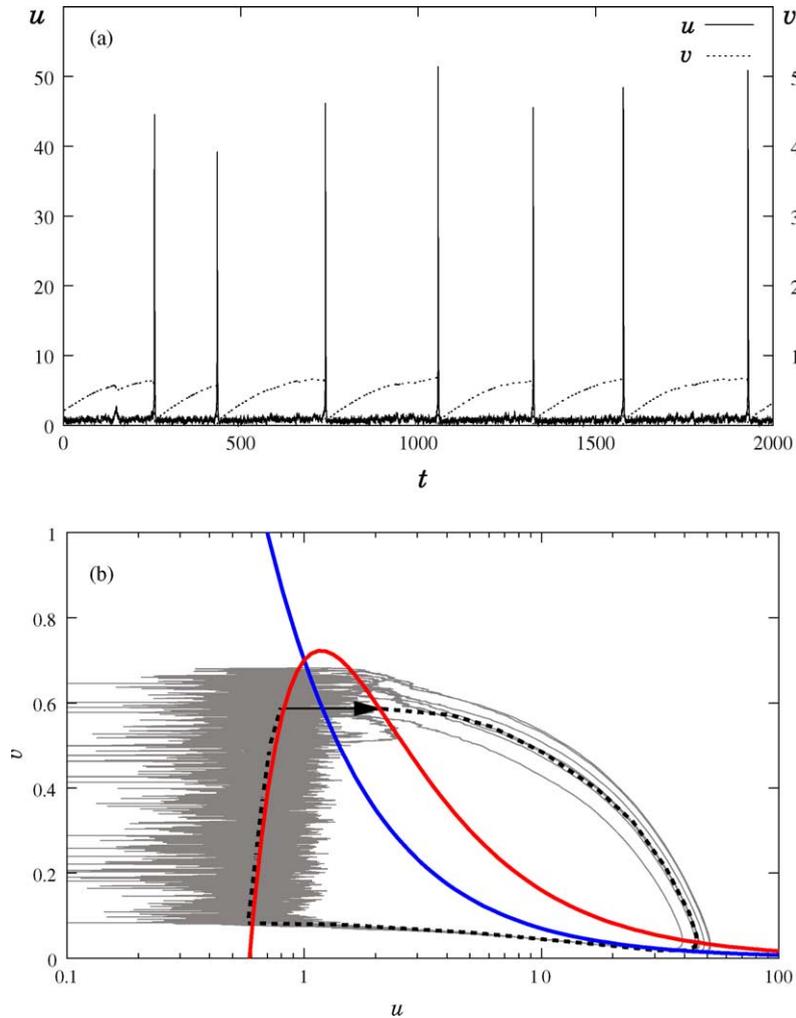
Fig. 2. Numerical solution of (6). The parameters are: $A = 0.7$, $\alpha = 0.01$, $\varepsilon = 0.1$. (a) The time series with the nearly periodic spike train. (b) The phase plane plot showing the corresponding (almost) deterministic limit cycle in gray. The thick solid lines are the u- and v-nullclines, respectively. The dashed line shows the predicted limit cycle, with the escape part shown by a solid line with an arrow. Note that the apparent size of the fluctuations of the trajectory around the slow manifold (stable branch of the u-nullcline) is accentuated by the logarithmic scale used for the variable u.

the parameters—later in Section 3.2 we perform simulations with different parameters. We use $\alpha = 0.01$, $\varepsilon = 0.1$ which are reasonably small values. We also take $A = 0.7$ which is not close to the Hopf bifurcation observed at $A_\omega \simeq 1$, see Eq. (8). We integrate Eq. (6) using a forward Euler scheme with adaptive time-step to fully resolve the fast excursion in the excited state. Fig. 2(a) shows the time series for one realization of the noise. This figure shows a train of large amplitude spikes in the excitatory variable. It is striking that the

spikes are occurring in an almost periodic fashion, with their amplitude and other characteristics being approximately the same at each time. This is corroborated by the phase plane portrait, Fig. 2(b), which shows a nearly limit cycle behavior in the u and v variables. The overall dynamics confirms the scenario in Section 2. A large excursion in the excited state is followed by a slow motion in the recovery state by which the system tries to go back to the steady state $(u_0, v_0) = (1, A)$. But it never succeeds as the noise systematically triggers new ex-
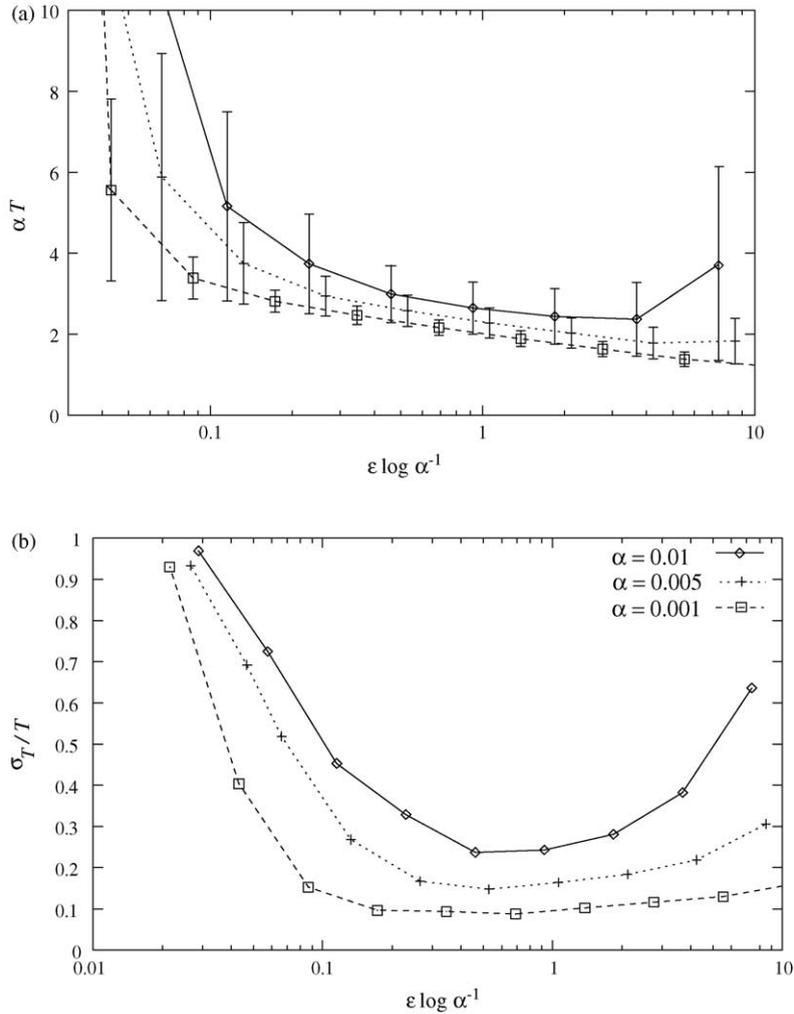
Fig. 3. The mean interspike distance T in (a) and its standard deviation σ_T in (b), as a function of the noise amplitude ε. Consistent with (4) we measure ε in units of $1/\log \alpha^{-1}$. In (a), the standard deviation is also shown as errorbars. In all cases $A = 0.7$, and the full curves correspond to the same value of α as in Fig. 2. Note the high degree of coherence that can be achieved when α is small, while at the same time T shows significant dependence on the noise amplitude ε.

cursions in the excited state before the system reaches (u_0, v_0). These excursions arise in a predictable fashion when v is around $v_\star < v_0$.

To further quantify the degree of coherence of the phenomenon, we have analyzed the statistics of the interspike time intervals as a function of the noise amplitude ε for different values of the time-scale separation ratio α. For the purpose of this analysis, we define as a spike any excursion with an amplitude $u_{max} \geq 10$. Fig. 3(a) shows the mean interspike interval T and its standard deviation σ_T obtained from the numerical so-

lution of Eq. (6). Also, in Fig. 3(b) we show the ratio σ_T/T, which characterizes the "signal-to-noise ratio" for the interspike distance.

For very small values of ε the spikes have the character of a Poisson process since $\sigma_T/T \to 1$ as $\varepsilon \to 0$ with α fixed (see the errorbar and Fig. 3(b)). They represent rare incoherent large-amplitude fluctuations away from the equilibrium point. Similarly it can be seen that for large noise amplitudes, when the noise is no longer weak, the spike train also looses coherence. However, the data plotted in Fig. 3(b) clearly show

that for the considered values of α there exists a broad range of ε where the ratio σ_T/T is low, signifying high degree of signal coherence (e.g., σ_T/T is less than 0.2 for $0.01 \leq \varepsilon \leq 1$ when $\alpha = 0.001$). Also, the degree of coherence increases as α decreases. At the same time, the value of T shows significant dependence on ε, while σ_T does not (as seen, e.g., from the errorbars).

3.1. Analysis

Now we present a quantitative explanation of these observations, consistent with the general scenario given in Section 2. Our analysis uses a combination between multiple-time perturbation techniques with matched asymptotics to describe the fast excitatory excursions and the slow recovery motion, and large deviation theory to describe the mechanism of escape from the slow manifold. The latter part of the analysis is complementary to the rigorous analysis performed by Freidlin in [2] on a different system and we refer the reader to this paper for more mathematical details.

3.1.1. Recovery state and escape
Suppose first that the noise is absent in Eq. (6), $\varepsilon = 0$. Then when $\alpha \ll 1$ the system relaxes quickly to $u = u_-(v)$, where $u_-(v)$ and $u_+(v)$ are the stable and the unstable branches of the u-nullcline, respectively. Solving $0 = 1 + u^2 v - (1 + A)u$ for u:

$$u_\pm(v) = \frac{1 + A \pm \sqrt{(1 + A)^2 - 4v}}{2v}, \tag{9}$$

and inserting $u_-(v)$ in the equation for v in Eq. (6) gives:

$$\dot{v} = \frac{2\alpha(A - v)}{1 + A - 2v + \sqrt{(1 + A)^2 - 4v}}. \tag{10}$$

Eq. (10) together with $u = u_-(v)$ specifies the slow recovery motion to leading order arising on the $O(\alpha^{-1})$ time-scale when $\alpha \ll 1$.

When the noise is present but small in amplitude, $\varepsilon \ll 1$, Eqs. (9) and (10) are not valid all the way up to (u_0, v_0) on the slow manifold (in fact, this point is never reached), but they still govern the slow recovery motion until the well-defined point $v_\star$ where escape from this slow manifold arises. To see this, let $\alpha \to 0$ in Eq. (6) assuming that u and v are $O(1)$. Then the equation for v reduces to $\dot{v} = 0$ which indicates that v

is frozen on the $O(1)$ fast-time scale, and on this time-scale, the dynamics is governed by the equation for u in Eq. (6) in which v enters as a fixed parameter. It is convenient to think of this equation as the motion of a particle in the potential, i.e. write it as:

$$\dot{u} = -\frac{\partial V(u, v)}{\partial u} + \sqrt{\varepsilon}\eta, \tag{11}$$

where $V(u, v)$ is given by:

$$V(u, v) = -\frac{1}{3}vu^3 + \frac{1}{2}(1 + A)u^2 - u \tag{12}$$

This potential is shown in Fig. 4 for different values of v. It has the shape of a left-slanted S, with a local minimum at $u = u_-(v)$, the intersection of $v = \text{const.}$ with the stable (left) branch of the u-nullcline defining the slow manifold and a local maximum at $u = u_+(v)$, the intersection of $v = \text{const.}$ with the unstable (right) branch of this nullcline. Therefore, even in the presence of a small noise, $\varepsilon \ll 1$, the system stays confined near this slow manifold and it can only escape via a noise-activated hopping event whose rate at given v has the form of Eq. (3) [6]:

$$k(v) = \frac{1}{2\pi}\sqrt{(1 + A)^2 - 4v} \, \exp\left(\frac{-\Delta V(v)}{\varepsilon}\right) \tag{13}$$

where $\Delta V(v) = 2[V(u_+(v), v) - V(u_-(v), v)]$ is explicitly given by:

$$\Delta V(v) = \frac{[(1 + A)^2 - 4v]^{3/2}}{3v^2}, \tag{14}$$

the energy barrier to be overcome. It is easy to check that $\Delta V(v)$ is a decreasing function of v on the entire interval $0 < v < (1 + A)^2/4$, i.e. the rate in Eq. (13), while very small when $\varepsilon \ll 1$, is a very rapidly increasing function of v. We can now apply the standard stochastic resonance argument recalled in Section 2. There is a precise value, $v = v_\star$, such that the rate matches the $O(\alpha)$ inverse time-scale on which the slow recovery motion governed by Eqs. (9) and (10) arises. Thus, Eq. (14) gives $\Delta V(v)$ to be inserted into Eq. (5), i.e.

$$\frac{[(1 + A)^2 - 4v_\star]^{3/2}}{3v_\star^2} = \beta \tag{15}$$

fixes $v_\star$ as a function of $\beta = \lim_{\varepsilon,\alpha \to 0} \varepsilon \log \alpha^{-1}$, and Eqs. (9) and (10) are only valid before v reaches $v_\star$.
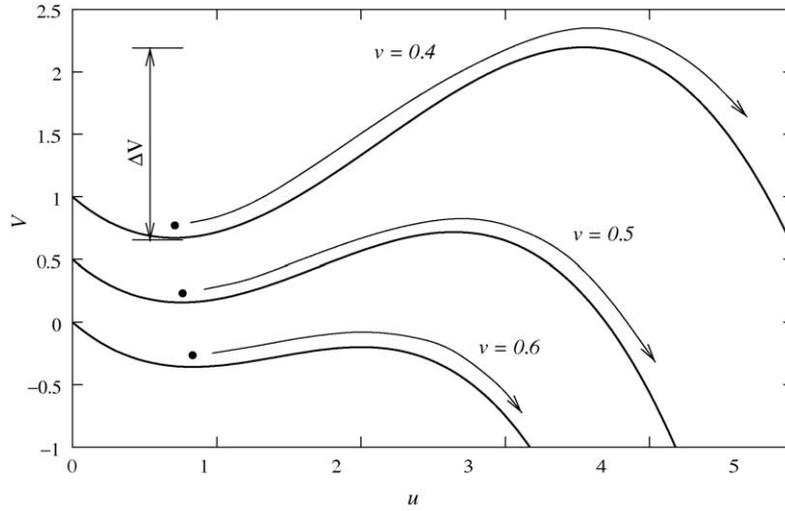
Fig. 4. The potential in (12), up to a constant, as a function of u for various values of v. The barrier decreases as v increases.

3.1.2. Excited state and reset

After the trajectory escapes the neighborhood of the stable nullcline at $v = v_\star$, it continues moving toward increasing values of u corresponding to the excited state. At this point the effect of the noise becomes negligible. With the increase of u, the effective time-scale of v decreases (see Eq. (6)), so when the system undergoes a large excursion in the excited state, the time-scales of these two variables can no longer be separated. On the other hand, when $u = O(\alpha^{-1})$ and $v = O(1)$, Eq. (6) can be simplified by neglecting all the terms except $u^2 v$. The resulting system of equations is:

$$\dot{u} = u^2 v \qquad \dot{v} = -\alpha u^2 v, \tag{16}$$

with the asymptotic boundary conditions $u(-\infty) = 0$, $v(-\infty) = v_\star$. This is equivalent to:

$$\dot{u} = u^2(v_\star - \alpha u), \qquad v = v_\star - \alpha u, \tag{17}$$

which can be solved exactly to give the transition layer for the rising part of the spike. It shows that in the spike u rises to $u_{\max} = \alpha^{-1} v_\star \gg 1$ on the time-scale of $\alpha \ll 1$, while v approaches zero asymptotically. This is then followed by a return to the recovery state, i.e.

the fall of the trajectory onto the u-nullcline with fixed $v = 0$ (asymptotically) according to:

$$\dot{u} = -(1 + A)u, \qquad v = 0. \tag{18}$$

with the asymptotic initial condition $u(0) = u_{\max}$.

Following the excursion in the excited state, the system starts over again the slow recovery motion governed asymptotically by Eqs. (9) and (10) with initial condition $v = 0$.

3.1.3. Characteristic of the limit cycle

Since the system spends most of the time on the slow manifold, asymptotically the period of the limit cycle will be equal to the time $T(v_\star)$ it takes to go from $v = 0$ to $v = v_\star$ by Eq. (10). This time is explicitly calculated by integrating Eq. (10):

$$T(v_\star) = \alpha^{-1} \left[A + v_\star - \sqrt{(1 + A)^2 - 4v_\star} + 1 + \frac{1}{2}(1 - A) \log \left(\frac{A^2(1 - A + \sqrt{(1 + A)^2 - 4v_\star})}{(A - v_\star)(A - 1 + \sqrt{(1 + A)^2 - 4v_\star})} \right) \right]. \tag{19}$$

Note also that β in Eq. (15) must satisfy:

$$\beta \in (\beta_c, \infty) \tag{20}$$

with

$$\beta_c = \frac{(1 - A)^3}{3A^2} = \frac{[(1 + A)^2 - 4v_0]^{3/2}}{3v_0^2} \tag{21}$$

since the attainable values of v on the u-nullcline lie in the interval $0 < v < v_0 = A$. In more colloquial terms, this means that for a fixed value of $\alpha \ll 1$ there is a critical amplitude of the noise for the establishment of the limit cycle behavior:

$$\varepsilon_c = \frac{(1-A)^3}{3A^2 \log \alpha^{-1}}. \tag{22}$$

No limit cycle behavior is possible when $\beta \le \beta_c$. As β approaches β_c from above, we have $v_\star \to v_0$, and $T(v_\star) \to \infty$. Therefore, if one fixes the parameters in the deterministic part of the dynamics there is a transition to a limit cycle behavior at a critical value of the amplitude of the noise.

Summarizing the results of this section, we have shown the feasibility of the mechanism of self-induced stochastic resonance on the specific example of the Brusselator. Small noise perturbations of the excitatory variable induce a transition to a deterministic limit cycle whose characteristics are controlled by the noise amplitude and the time-scale ratio according to the value of $\beta = \lim_{\varepsilon,\alpha \to 0} \varepsilon \log \alpha^{-1}$. The limit cycle is established away from the bifurcation, i.e. for values of A which do not need to be close to the critical value $A_\omega \to 1$ as $\alpha \to 0$, see Eq. (8). On the other hand, the limit cycle is observed only if the noise is above the critical value given by Eq. (22). We now proceed to corroborate these predictions via further numerical experiments.
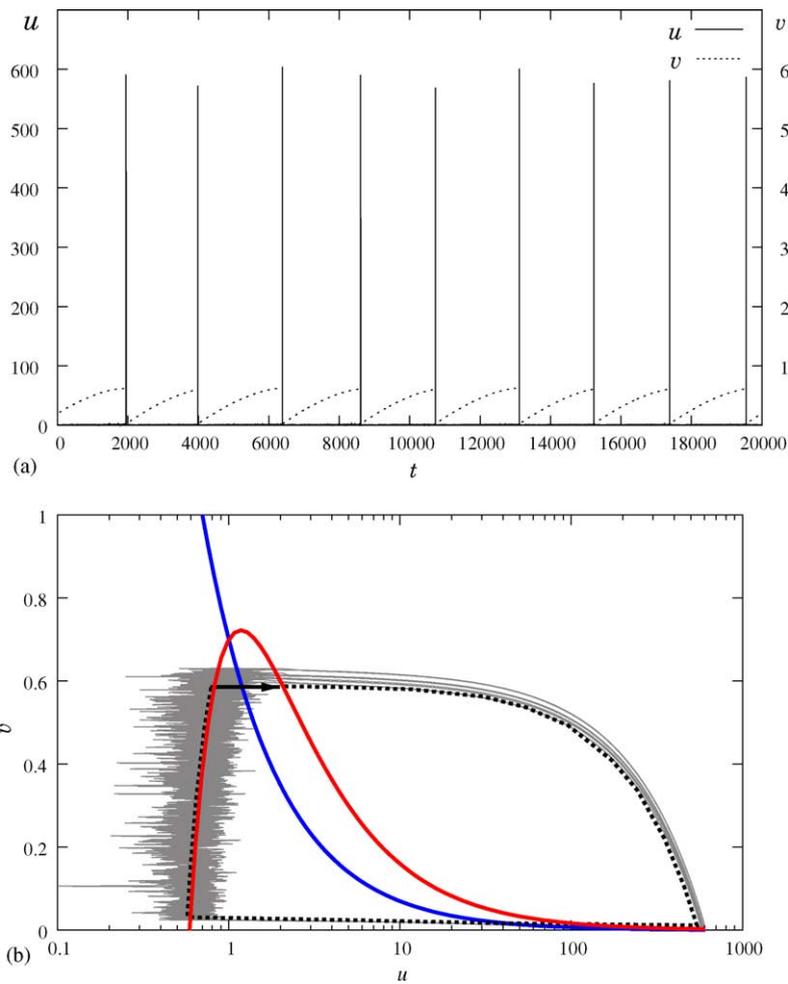

Fig. 5. Numerical solution of the stochastic differential equation for $\alpha = 0.001$, $\varepsilon = 0.067$, $A = 0.7$. The nullclines are shown with thick solid lines, the predicted limit cycle is shown by the dashed line, with the escape part shown by a solid line with an arrow.

3.2. Numerical validation

Since the proposed mechanism operates in the limit $\alpha, \varepsilon \to 0$, with the value of $\varepsilon \log \alpha^{-1}$ fixed, we performed further numerical studies of the model at smaller values of the parameter α to verify its predictions. Our first simulation was performed at the same values of A and $\varepsilon \log \alpha^{-1}$ as in Fig. 2, but with $\alpha = 0.001$, an order of magnitude smaller. The results are shown in Fig. 5. From this figure, one can see a significant improvement of coherence (the computed value of $\sigma_T / T \simeq 0.08$ here), in agreement with our prediction that the coherence becomes perfect in the limit $\alpha \to 0$. Also, the mean interspike interval T is now
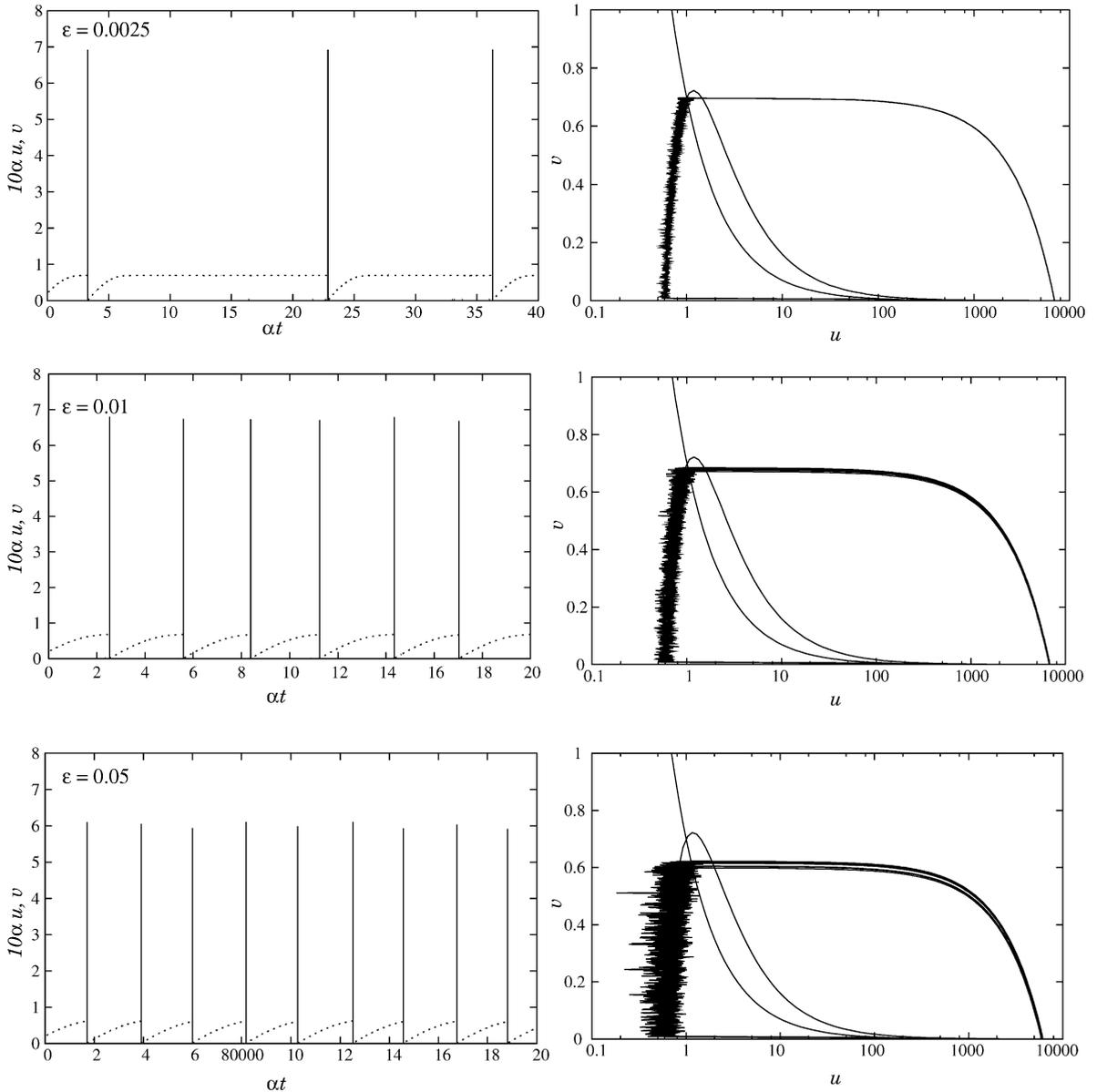

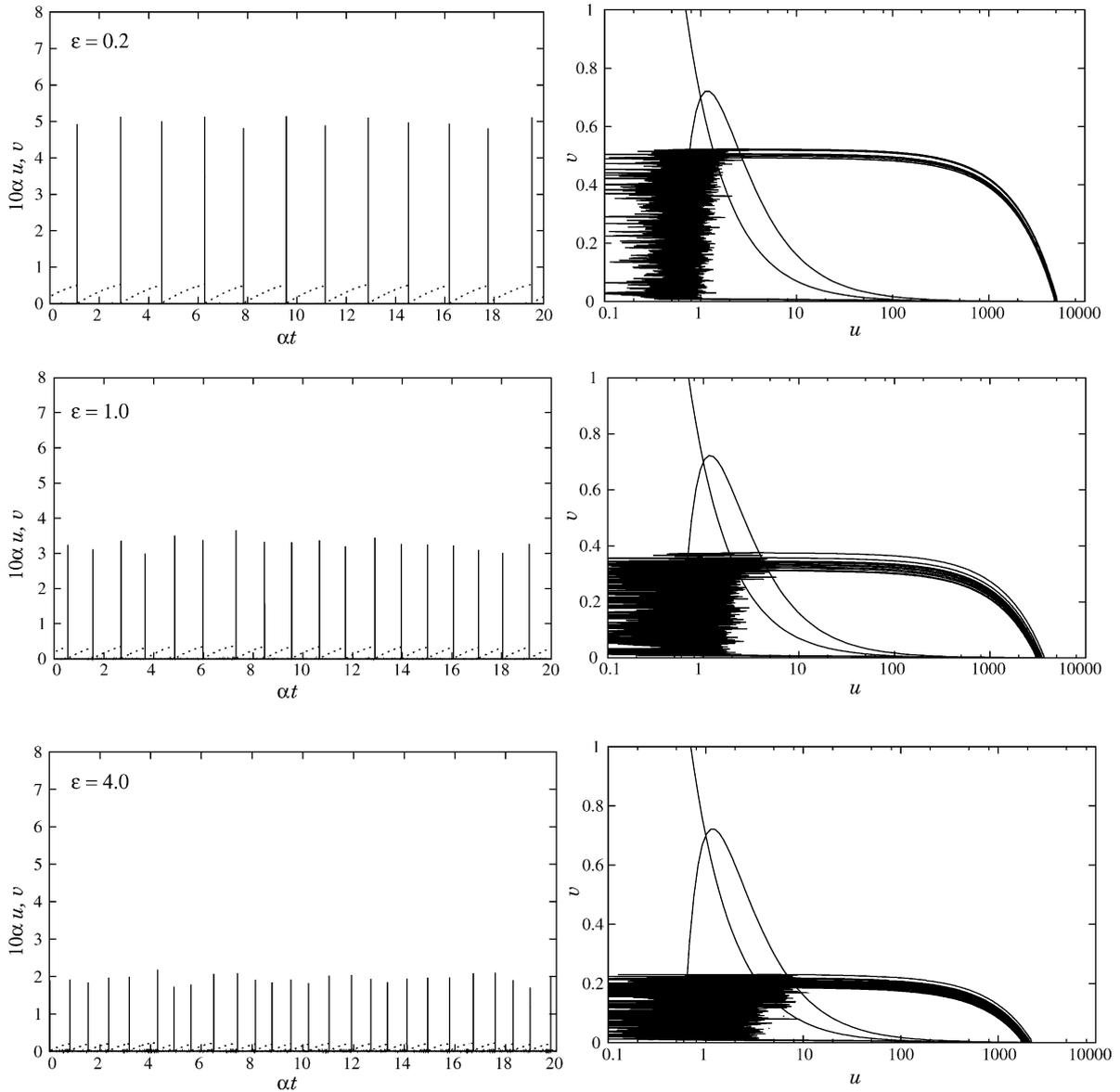Fig. 6. The effect of varying the noise amplitude: results of the simulations at $\alpha = 0.0001$, $A = 0.7$.

Fig. 7. The effect of varying the noise amplitude (continued): results of the simulations at $\alpha = 0.0001$, $A = 0.7$. (Recall that the apparent size of the fluctuations around the stable branch of the u-nullcline is accentuated by the logarithmic scale we use for u.)

within $\sim 20\%$ of the value given by Eq. (19). Simulations show that decreasing α further consistently improves the agreement with the theory (we verified this down to $\alpha = 10^{-6}$).

We next investigate the effect of varying the noise amplitude on the parameters of the limit cycle. The simulations are performed at $\alpha = 0.0001$ and $A = 0.7$

and are shown in Figs. 6 and 7. Our first prediction is that for $\varepsilon < \varepsilon_c$, which in the limit $\alpha \to 0$ is given by Eq. (22), no coherent oscillations will exist. This is what we observe in the simulations when $\varepsilon \lesssim 0.0025$, see the first row in Fig. 6. Here, instead of a periodic spike train we observe a Poisson sequence of spikes. On the other hand, at $\varepsilon = 0.003$ the behavior rather abruptly

changes to almost periodic, consistent with our theory (for this value of α the predicted value of $\varepsilon_c = 0.002$, within reasonable agreement with the observations).

Increasing the noise amplitude, we see that the period and the amplitude of the observed periodic limit cycle decreases, while the spike train maintains a high degree of coherence, see the two lower panels of Fig. 6. One can also see from the phase portrait in the lower panel of Fig. 6 that the trajectory leaves the u-nullcline at a particular point below the equilibrium (u_0, v_0) via a noise-activated process, consistent with our mechanism. This is seen more dramatically at larger values of ε, see Fig. 7. Clearly, the location of the equilibrium has no effect on the value of $v_\star$ at which

the trajectory escapes the u-nullcline. Remarkably, however, the limit cycle maintains its coherence even for $\varepsilon = 4$ (then the noise is no longer weak, but $\Delta V(v_\star)/\varepsilon$ is still large, which suffices for our theory to apply). One can also clearly see that noise indeed controls the parameters of the limit cycle. For example, the period and the amplitude of the limit cycle changes several-fold in the simulations in Figs. 6 and 7, while the degree of coherence is essentially unchanged. In other words, the noise amplitude really acts as a control parameter for the oscillatory behavior of the system.

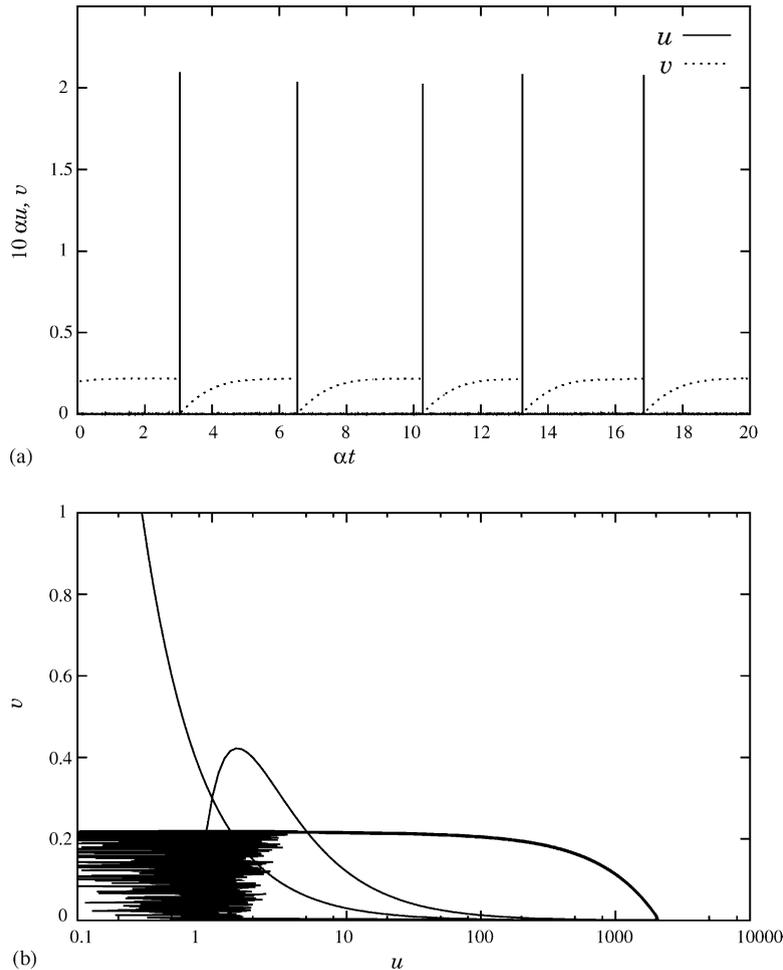Finally, we verify the robustness of our mechanism by showing that it does not require tuning of the param-

Fig. 8. Tuning is not required for the mechanism: results of the simulation at $\alpha = 0.0001$, $A = 0.3$, $\varepsilon = 0.6$.

eters and can be realized far from bifurcation points. To this end, we take $\alpha = 0.0001$ and $A = 0.3$, which is about three times smaller than A_ω. The results of the simulation with $\varepsilon = 0.6$ are shown in Fig. 8. Note that for these values of A one needs stronger noise to induce the oscillations (for example, the predicted value of ε_c at these parameters is $\varepsilon_c \simeq 0.14$). Once again, we see a coherent almost periodic spike train, with a clearly defined value of $v_\star$ which is significantly lower than v_0, consistent with our theory.

4. Comparison with coherence resonance

As explained before, self-induced stochastic resonance arises away from the Hopf bifurcation at $A = A_\omega$ and the limit cycle it induces can be controlled by the parameter $\beta = \lim_{\varepsilon, \alpha \to 0} \varepsilon \log \alpha^{-1} \in (\beta_c, \infty)$ (recall that the constraint $\beta > \beta_c$ guarantees that the system hops out of the slow manifold of the recovery state and back into the excited state before reaching the steady state). Self-induced stochastic resonance persists in the limit as $A \to 1$, which is the limiting value of A_ω as $\alpha \to 0$ (see Eq. (8)), provided that $\beta > 0$ in this limit (in fact, this is true even when $A > 1$). However, as $A \to 1$, a limit cycle can also be established when $\beta = 0$, but by a mechanism different from ours and closer to coherence resonance.

Indeed, suppose that $A \to 1^-$ first and then let $\alpha, \varepsilon \to 0$ in a way that $\beta = \lim_{\alpha, \varepsilon \to 0} \varepsilon \log \alpha^{-1} = 0$. In this limit, the steady state is $(u_0, v_0) = (1, 1)$, the point located at the top of the u-nullcline, which is neutrally stable. Starting from $v = 0$, integrating Eq. (10) shows that the deterministic trajectory reaches the top of this nullcline in finite time $T = T_\omega$, where

$$T_\omega = 3\alpha^{-1}. \tag{23}$$

Since $\beta = 0$, the noise is too weak to make the trajectory hop from the u-nullcline before it reaches (u_0, v_0). But once the trajectory reaches (u_0, v_0), since there is no energy barrier to overcome to escape this point, a vanishingly small amount of noise allows the trajectory to take off and perform a large excursion in the excited state described by Eqs. (17) and (18), then return back to $v = 0$ on the u-nullcline and complete the cycle.

Since the motion described by Eq. (17) and (18) is much faster than the one described by Eq. (10) which

led to Eq. (23), the period of the limit cycle is given by T_ω in the limit as $\alpha \to 0$. It is also clear that T_ω will be the period of the emerging limit cycle as $A \to 1^+$. So, the noise plays a rather passive role in this mechanism of coherence resonance since the limit cycle induced by noise right before bifurcation is essentially the same as the one that will be established right after bifurcation, and its period T_ω given in Eq. (23) depends on α only and not on ε.

5. Concluding remarks

In summary, we have shown that a vanishingly small noise in excitable systems with strong time-scale separation can induce a transition to a limit cycle behavior. The mechanism, which we term self-induced stochastic resonance, is robust as it arises away from bifurcations, and it leads to a limit cycle whose period and amplitude can be controlled by the noise. This is different from other mechanisms like coherence resonance which are less robust as they require the system to be close to bifurcation and lead to a limit cycle which is essentially the same as the one that emerges after bifurcation and cannot be controlled by the noise.

We believe that self-induced stochastic resonance may have important implications in several areas. Consider for instance, coupled excitable systems. Our analysis indicates that in such systems the level of the noise, both extrinsic and intrinsic, may be used as an information carrier and be transformed into a (quasi-)deterministic signal. As a prototype, consider a system of all-to-all positively coupled excitable cells. Under the action of the noise of sufficiently small amplitude each cell will occasionally generate a spike. These spikes will have random phases, so their total input on each individual cell may average to a stationary random signal of low intensity. Now, if the noise level suddenly increases due to an external disturbance, the cells may switch to the noise-assisted oscillatory mode. This will further increase the effective noise amplitude, so that the oscillatory mode may persist even after the disturbance is removed. In colloquial terms, the system in a dormant state may wake up from the outside rattle.

In a similar way, our results may be applied to spatially distributed excitable media [9]. In these systems the analog of the noise-activated event will be the for-

mation of a radially symmetric nucleus, leading to subsequent initiation of radially divergent waves [9,10,12]. In the wake of such a wave the system will undergo recovery. It is clear, then, that the system will be most recovered at the position where the wave was initiated. Hence, the new wave will be initiated again at the same spot, with the dynamics repeating periodically. This suggests that the well-known phenomenon of target pattern formation in two-dimensional excitable media [9] might have an alternative interpretation in terms of noise-driven periodic wave generation.

Acknowledgements

References

[1] M.I. Freidlin, Quasi-deterministic approximation, metastability and stochastic resonance, Physica D 137 (2000) 333–352.

[2] M.I. Freidlin, On stable oscillations and equilibriums induced by small noise, J. Stat. Phys. 103 (2001) 283–300.

[3] M.I. Freidlin, A.D. Wentzell, Random Perturbations of Dynamical Systems, Springer-Verlag, New York, 1984.

[4] L. Gammaitoni, P. Hänggi, P. Jung, F. Marchesoni, Stochastic resonance, Rev. Mod. Phys. 70 (1998) 223–287.

[5] H. Gang, T. Ditzinger, C.Z. Ning, H. Haken, Stochastic resonance without external periodic force, Phys. Rev. Lett. 71 (1993) 807–810.

[6] C.W. Gardiner, Handbook of Stochastic Methods for Physics, Chemistry and the Natural Sciences, Springer-Verlag, Berlin, 1985.

[7] J. Keener, J. Sneyd, Mathematical Physiology, Springer-Verlag, New York, 1998.

[8] B. Lindner, J. Garcia-Ojalvo, A. Neiman, L. Schimansky-Geier, Effects of noise in excitable systems, Phys. Rep. 392 (2004) 321–424.

[9] A.S. Mikhailov, Foundations of Synergetics, Springer-Verlag, Berlin, 1990.

[10] C.B. Muratov, V.V. Osipov, Spike autosolitons and pattern formation scenarios in the two-dimensional Gray-Scott model, Eur. Phys. J. B 22 (2001) 213–221.

[11] G. Nicolis, I. Prigogine, Self-Organization in Non-Equilibrium Systems, Wiley Interscience, New York, 1977.

[12] V.V. Osipov, C.B. Muratov, Ultrafast traveling spike autosolitons in reaction–diffusion systems, Phys. Rev. Lett. 75 (1995) 338–341.

[13] A.S. Pikovsky, J. Kurths, Coherence resonance in a noise-driven excitable system, Phys. Rev. Lett. 78 (1997) 775–778.

[14] T. Wellens, V. Shatokhin, A. Buchleitner, Stochastic resonance, Rep. Prog. Phys. 67 (2004) 45–105.

[15] M.P. Zorzano, L. Vázquez, Emergence of synchronous oscillations in neural networks excited by noise, Physica D 179 (2003) 105–114.